CVEL

THE CLEMSON UNIVERSITY VEHICULAR ELECTRONICS LABORATORY

TECHNICAL REPORT: CVEL-11-027

Special Considerations for PCB Heatsink Radiation Estimation

Xinbo He and Dr. Todd Hubing
Clemson University

May 4, 2011

Table of Contents

Abstract

At frequencies where heatsink dimensions are comparable to a wavelength, the radiated emissions from a heatsink-PCB geometry can be high enough to cause EMI problems. Although full-wave software can be applied to this problem, it is desirable to have a method that can be more easily and intuitively used to estimate the maximum possible emissions from a given heatsink-PCB geometry. A practical method has been proposed in a previous report [6] to estimate the maximum radiated emissions from a heatsink given the maximum voltage along the bottom edge. This report describes modeling and measurement results that support the previous study, but were too detailed or redundant to include in that report. These results include a measurement of the voltage along the edge of a practical heatsink; the influence of the heatsink fins on the estimation; validation of the estimated 30 - 40 ohm radiation resistance for thick monopoles; estimation of the heatsink resonance frequency; and more simulation results to validate the heatsink radiation estimate for different heatsink geometries.

1. Configuration for measuring the heatsink driving voltage

To measure the voltage along the heatsink edge, a probe is needed. In this study, the probe was an SMA coax connector (with a characteristic impedance of 50 ohm) with a 1-k□ resistor between the cable core conductor and the heatsink. The shield of the cable connector is connected to the circuit board ground. This configuration is illustrated in Fig. 1 below.

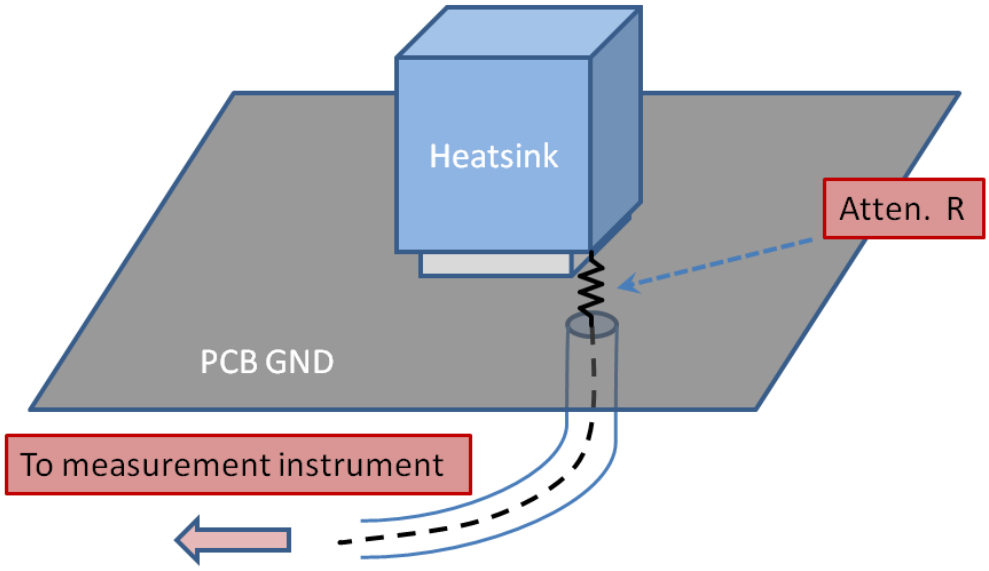

Fig. 1. Measurement of heatsink driving voltage along the bottom edges.

With this configuration, the driving voltage can be measured using a spectrum analyzer or other instruments. Then the data obtained can be used with the estimation formula to obtain the estimated maximum radiated emissions from a specific heatsink. The driving voltage at the measurement port can be calculated from the measured voltage as,

$$V_{Heatsink} = \frac{R+50}{50} \times V_{Measurement}, \quad (1)$$

2. Influence of Fin Structures on Heatsink Radiated Emissions

Earlier research [1] [2] [3] models the heatsink as a conductive metal block. The fine features of the fins are neglected. No specific validation was provided to justify this simplification. In order to verify the assumption that the fins have little influence on the maximum heatsink radiation, some simulation and measurements were conducted and are described below.

Two heatsinks were studied, which have the dimensions listed in Table I. One heatsink is relatively short and the other relatively tall. The radiated emissions 3 meters away from the heatsinks mounted on a large PEC ground were measured in a semi-anechoic chamber and simulated using full-wave electromagnetic modeling software [4].

Table I. Two heatsinks used in the study.

	Short heatsink	Tall heatsink
Length (L) mm	90	66
Width (W) mm	70	40
Height (H) mm	15	55
Cavity height (S) mm	3	3

The heatsink was driven by a coaxial connector through the copper plane 5 x 5 mm off center on the bottom face of the heatsink.

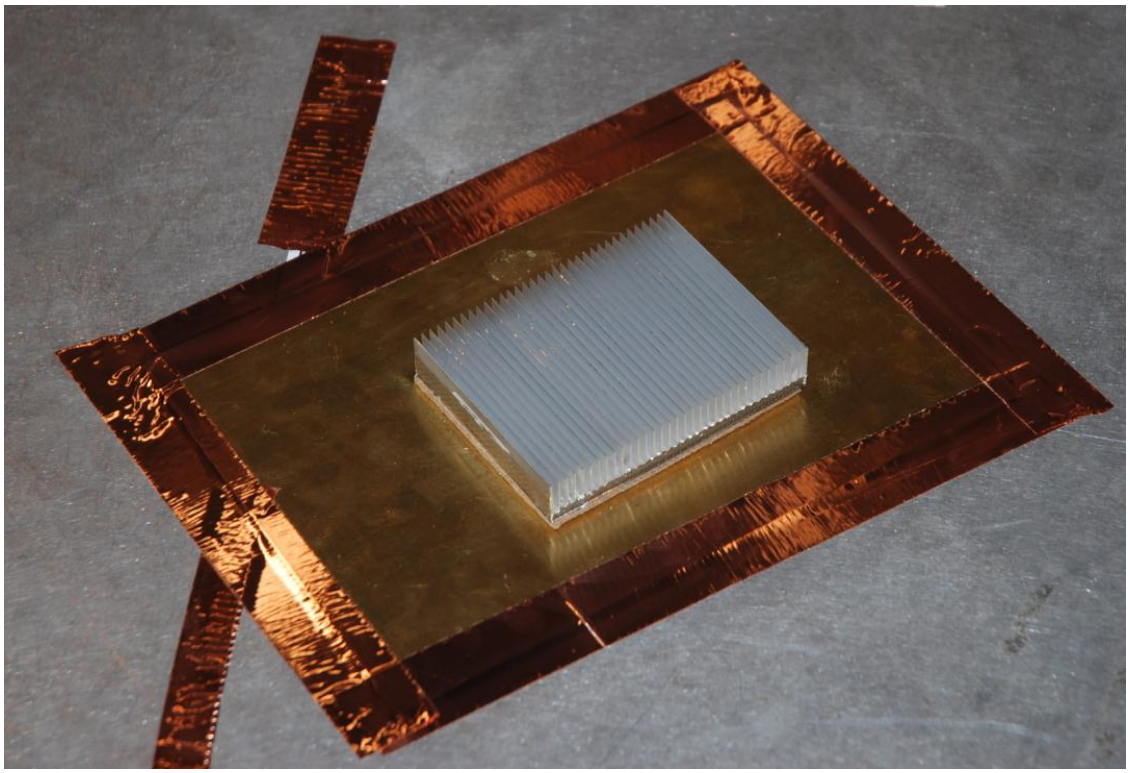

Fig. 2. Measurement of the short heatsink with fins.

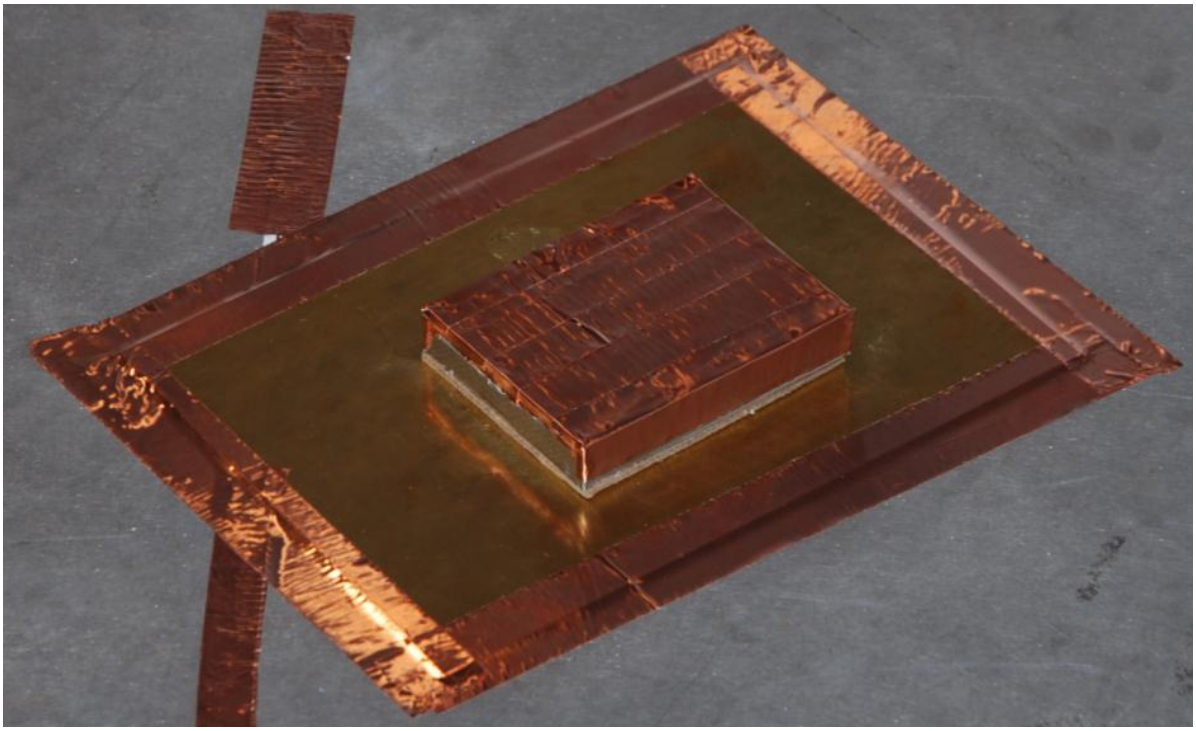

Fig. 3. Measurement of the short heatsink without fins.

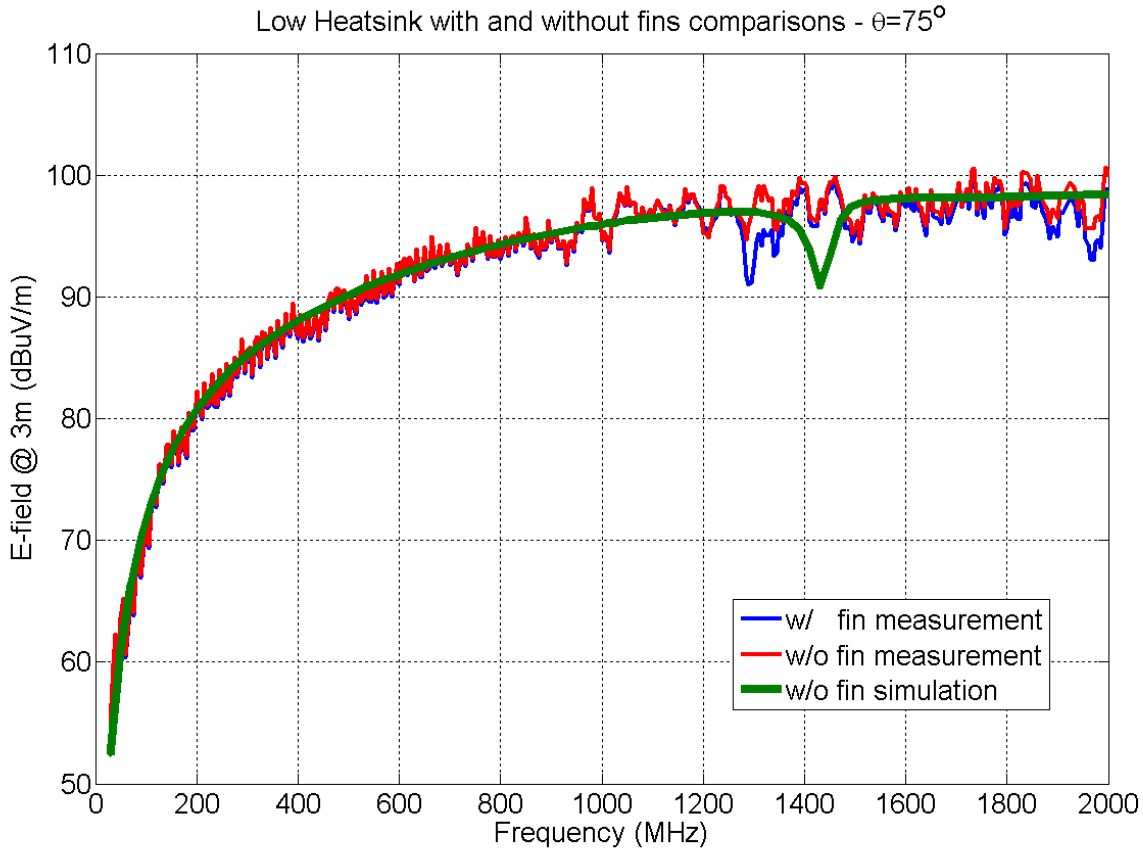

Fig. 4. Measurement and simulation results of the short heatsink.

Fig. 2 shows the measurement setup for the short heatsink with fins, and Fig. 3 shows the measurement configuration for the short heatsink with no fins. In Fig. 3 the same heatsink as that in Fig. 2 is used. To remove the effects of the fins, conductive copper tape was used to cover all the fins. Thus the heatsink looks like a rectangular conductive block.

Fig. 4 shows the measured electric field from the heatsink 3 meters away and 1 meter above the infinite ground. In the same figure, the measured and simulated radiated electric field at the same position from the short heatsink without fins is also plotted. It is apparent that for the frequencies from 30 MHz up to 2 GHz the two measurements have very good agreement. Furthermore, there is good agreement between the measurements and the simulated results.

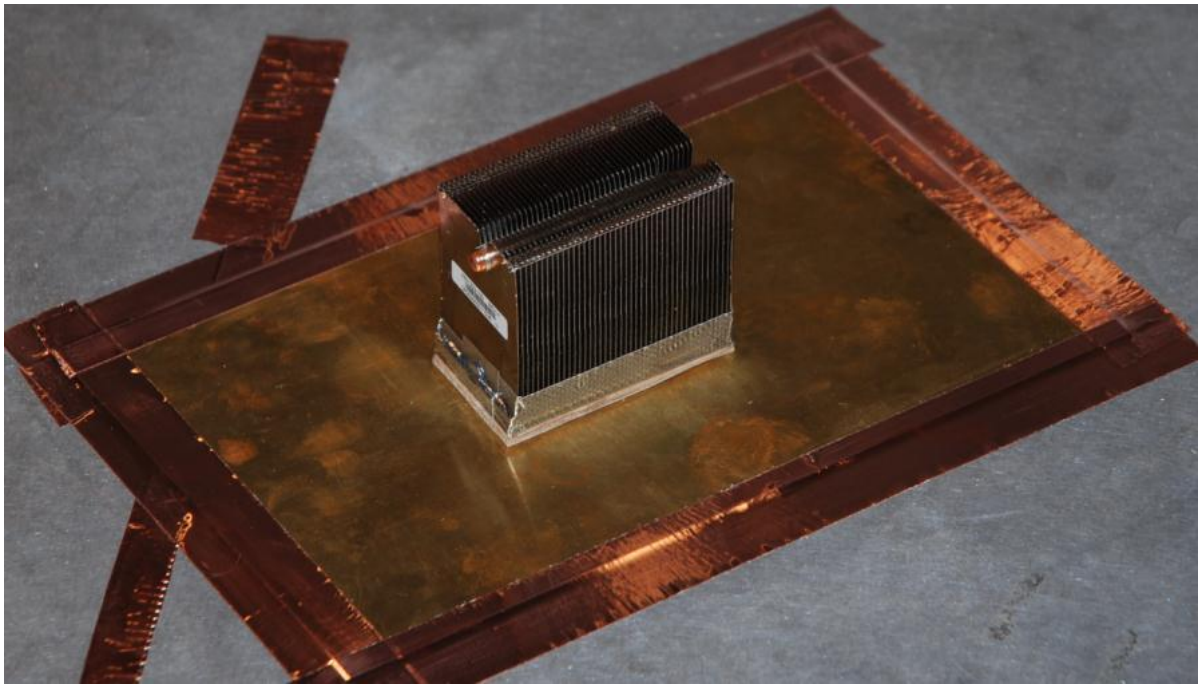

Fig. 5. Measurement of the tall heatsink with fins.

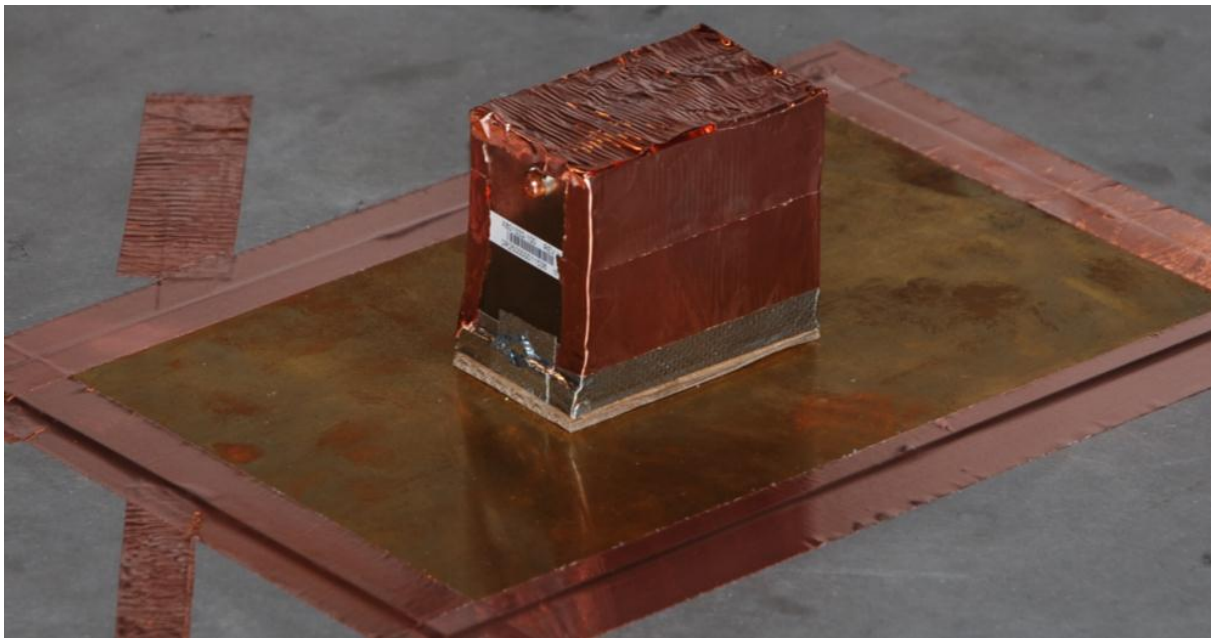

Fig. 6. Measurement of the tall heatsink without fins.

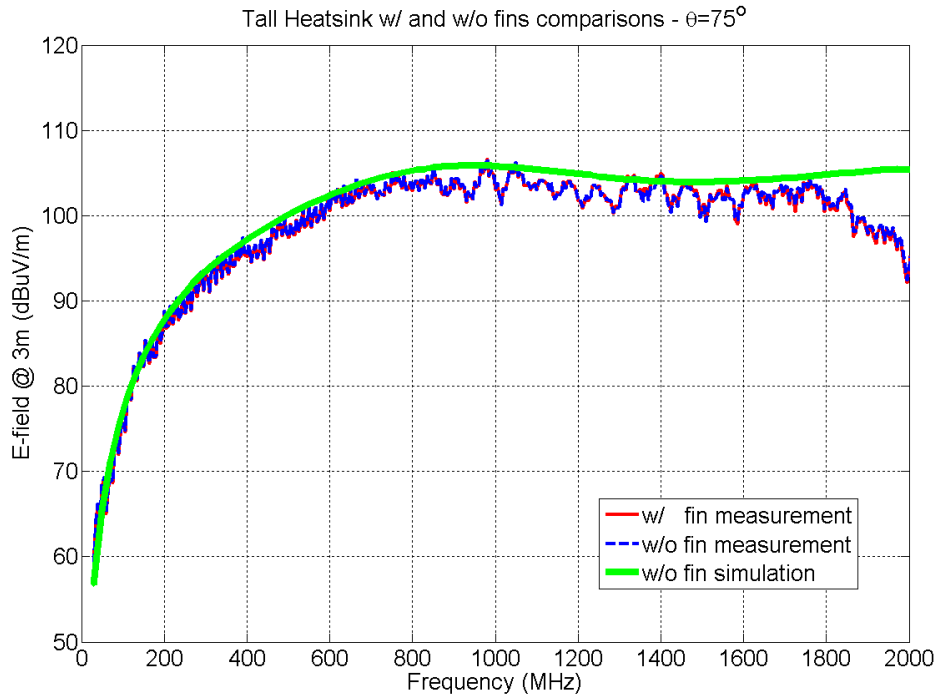

Fig. 7. Measurement and simulation results of the tall heatsink.

Fig. 5 shows the measurement setup for the tall heatsink with fins, and Fig. 6 shows the measurement configuration for the tall heatsink without fins. To remove the effects of the fins, conductive copper tape was used to cover all the fins..

Fig. 7 shows the measured electric field from the heatsink 3 meters away and 1 meter above the infinite ground. In the same figure, the measured and simulated radiated electric field, at the same position from the tall heatsink without fins is also plotted. From 30 MHz up to 2 GHz, the measurements agree very well. Furthermore, there is reasonable agreement between the measurements nd the simulation results.

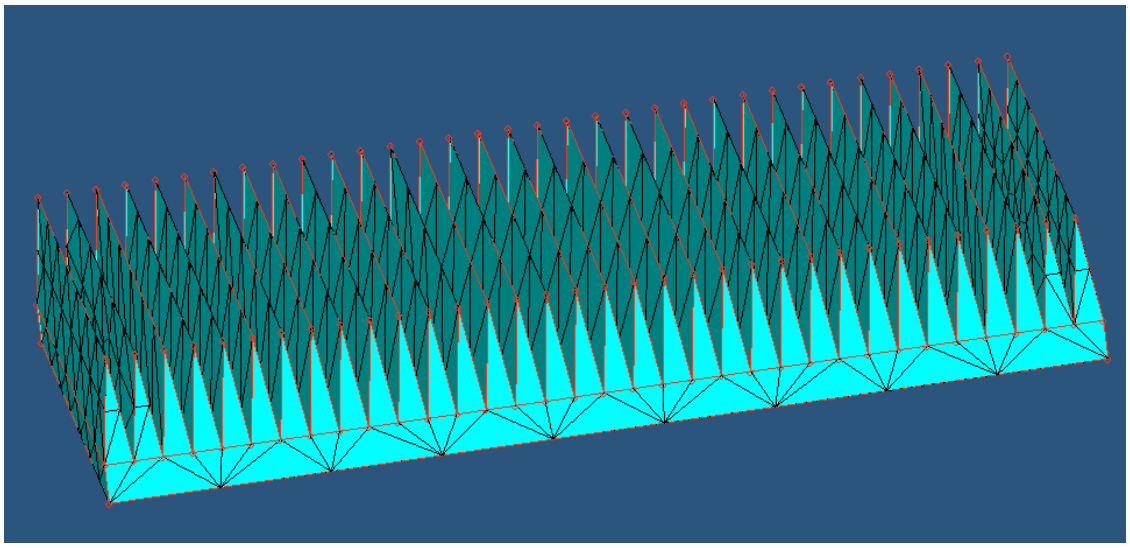

Fig. 8. Simulation of the short heatsink with fins.

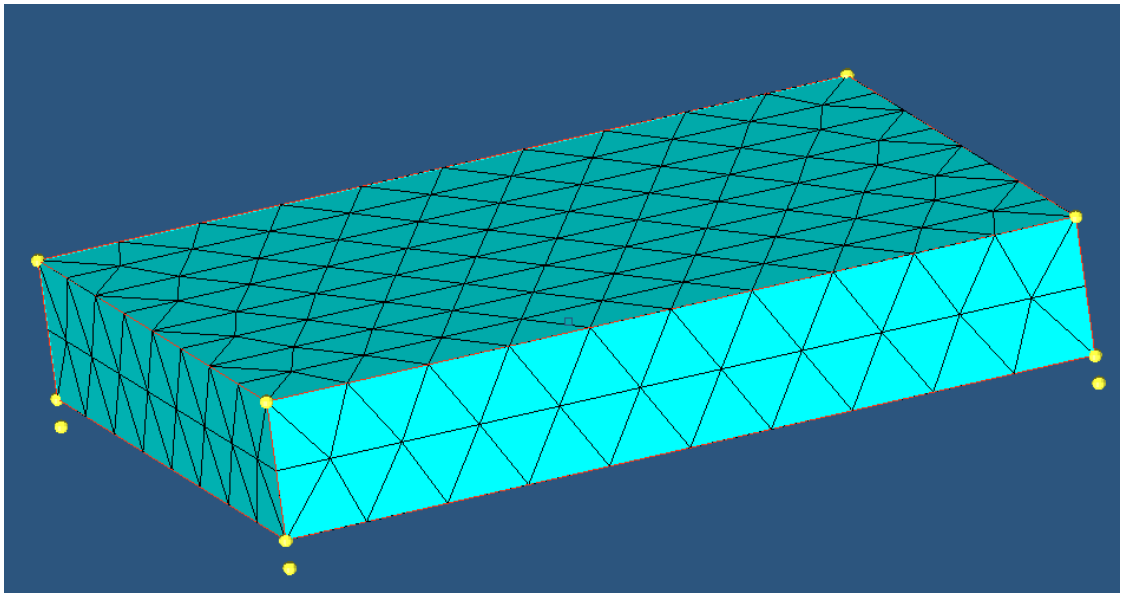

Fig. 9. Simulation of the short heatsink without fins.

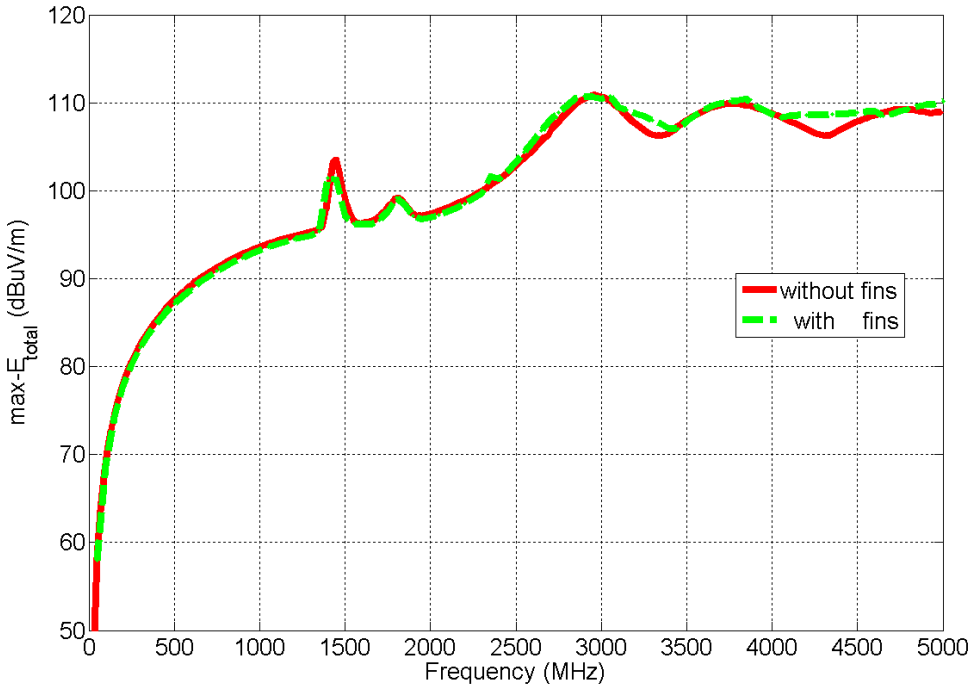

Fig. 10. Simulated maximum radiated emissions of the short heatsink with and without fins.

In the previous measurements, the radiated electric field was only measured at one position. Restricted by the measurement conditions, the maximum radiated emissions in the whole spatial volume at every frequency could not be obtained. To study the influence of the heatsink fins on the maximum radiated emissions, full-wave simulations were performed.

Two full-wave simulations were done: one with all 34 fins featured (Fig. 8) and the other with the fins replaced by a conductive block (Fig. 9). The outer dimensions of the two heatsink models are the same. Fig. 10 shows the maximum radiated electric field 3 meters away from the two heatsinks. For frequencies from 10 MHz to 5 GHz, the two results are very close.

3. Thick Cylindrical Monopole Radiation Resistance

From [5] a cylindrical dipole has a radiation resistance of 67 ohms at the first resonance, and a cylindrical monopole has a radiation resistance of 34 ohms at the first resonance. To verify whether this can be used for a thick monopole-like heatsink above a relatively large ground, some full-wave simulations were performed.

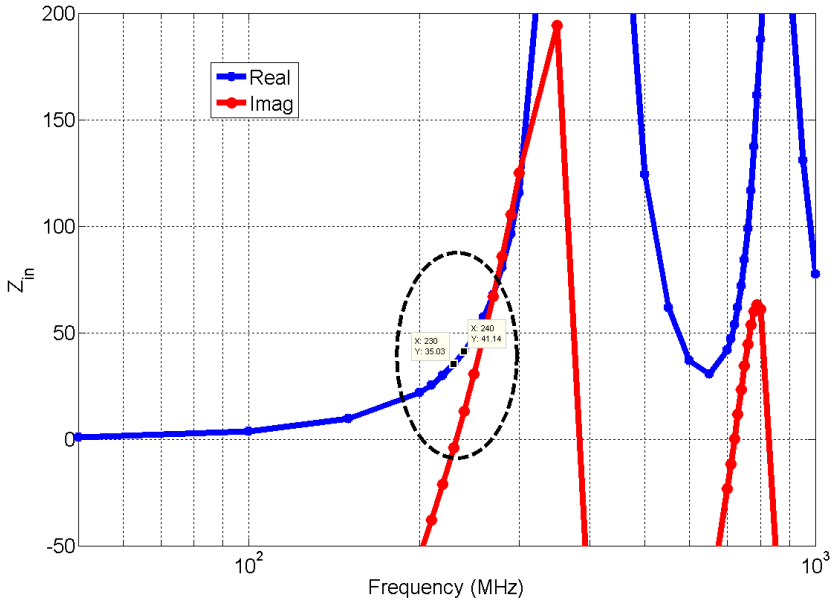

Fig. 11. Input impedance of a tall heatsink model with length 4.5 mm, width 3.2 mm, height 305 mm, and cavity spacing 1 mm.

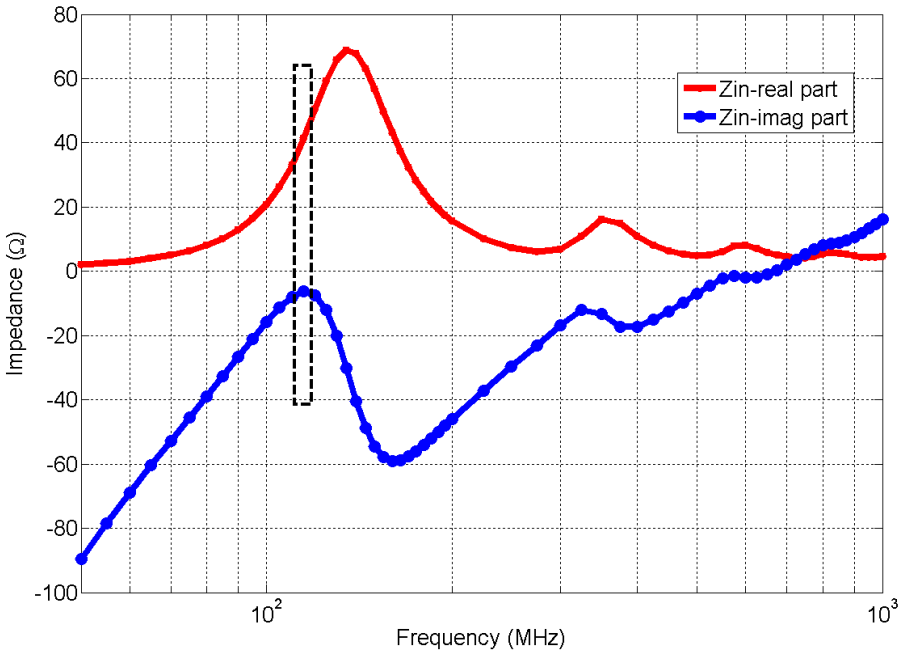

Fig. 12. Input impedance of a heatsink with length 90 mm, width 64 mm, height 600 mm, and cavity spacing 6 mm.

From Fig. 11, the radiation resistance of a relatively tall heatsink is between 35 and 40 ohms. From Fig. 12, a relatively tall heatsink has a radiation resistance of about 40 ohms at the first resonance. For a heatsink with a height less than its length or width, cavity resonances (associated with the cavity formed between the heatsink and circuit board) will affect the currents at the source and it is difficult to determine the input impedance of the heatsink body.

4. Validation of Method for Estimating Maximum Heatsink Radiation

In [6], the following equations were derived for calculating the maximum radiated emissions from a heatsink-PCB geometry given the maximum voltage between the heatsink and PCB at the base of the heatsink:

$$\frac{|E|_{\max}}{|V|_{\max}} = \begin{cases} \dfrac{k^2 LW}{\pi r} + \left(\dfrac{k}{k_{hs}}\right)^2 \dfrac{60}{rR_{res}} & k \le k_{hs} \\ \dfrac{k^2 LW}{\pi r} + \dfrac{60}{rR_{res}} & k_{hs} < k \le \dfrac{2}{L} \\ \dfrac{kW}{\pi r} + \dfrac{60}{rR_{res}} & \dfrac{2}{L} < k \le \left(\dfrac{\pi}{W} + \dfrac{\pi p}{L}\right)/2 \\ \dfrac{L}{rW} + \dfrac{60}{rR_{res}} & k > \left(\dfrac{\pi}{W} + \dfrac{\pi p}{L}\right)/2 \end{cases} \qquad k_{hs} \le \frac{2}{L} \tag{2a}$$

$$\frac{|E|_{\max}}{|V|_{\max}} = \begin{cases} \dfrac{k^2 LW}{\pi r} + \left(\dfrac{k}{k_{hs}}\right)^2 \dfrac{60}{rR_{res}} & k \le \dfrac{2}{L} \\ \dfrac{kW}{\pi r} + \left(\dfrac{k}{k_{hs}}\right)^2 \dfrac{60}{rR_{res}} & \dfrac{2}{L} < k \le k_{hs} \\ \dfrac{kW}{\pi r} + \dfrac{60}{rR_{res}} & k_{hs} < k \le \left(\dfrac{\pi}{W} + \dfrac{\pi p}{L}\right)/2 \\ \dfrac{L}{rW} + \dfrac{60}{rR_{res}} & k > \left(\dfrac{\pi}{W} + \dfrac{\pi p}{L}\right)/2 \end{cases} \qquad \frac{2}{L} < k_{hs} \le \left(\frac{\pi}{W} + \frac{\pi p}{L}\right)/2 \tag{2b}$$

$$\frac{|E|_{\max}}{|V|_{\max}} = \begin{cases} \dfrac{k^2 LW}{\pi r} + \left(\dfrac{k}{k_{hs}}\right)^2 \dfrac{60}{rR_{res}} & k \le \dfrac{2}{L} \\ \dfrac{kW}{\pi r} + \left(\dfrac{k}{k_{hs}}\right)^2 \dfrac{60}{rR_{res}} & \dfrac{2}{L} < k \le \left(\dfrac{\pi}{W} + \dfrac{\pi p}{L}\right)/2 \\ \dfrac{L}{rW} + \left(\dfrac{k}{k_{hs}}\right)^2 \dfrac{60}{rR_{res}} & \left(\dfrac{\pi}{W} + \dfrac{\pi p}{L}\right)/2 < k \le k_{hs} \\ \dfrac{L}{rW} + \dfrac{60}{rR_{res}} & k > k_{hs} \end{cases} \qquad k_{hs} > \left(\frac{\pi}{W} + \frac{\pi p}{L}\right)/2 \tag{2c}$$

In Figs. 13-26, estimates obtained using these equations are compared to full-wave simulation results for various heatsink-PCB geometries.

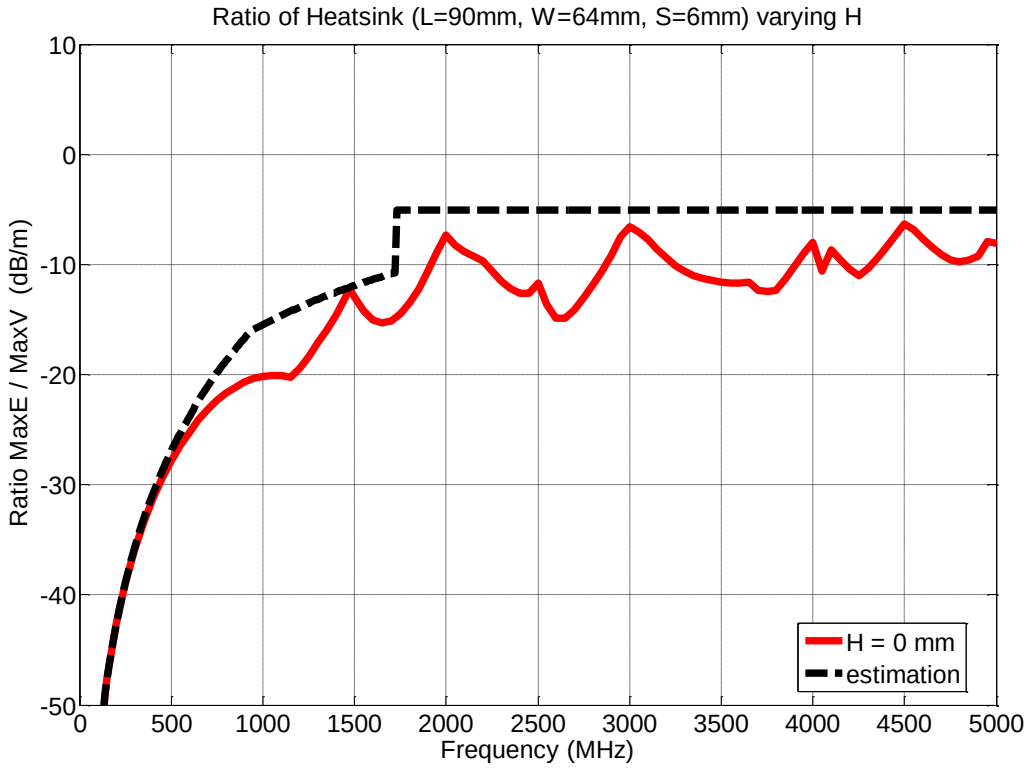

Fig. 13. Emissions from heatsink with dimensions: L=90 mm, W=64 mm, S= 6 mm and H=0 mm.

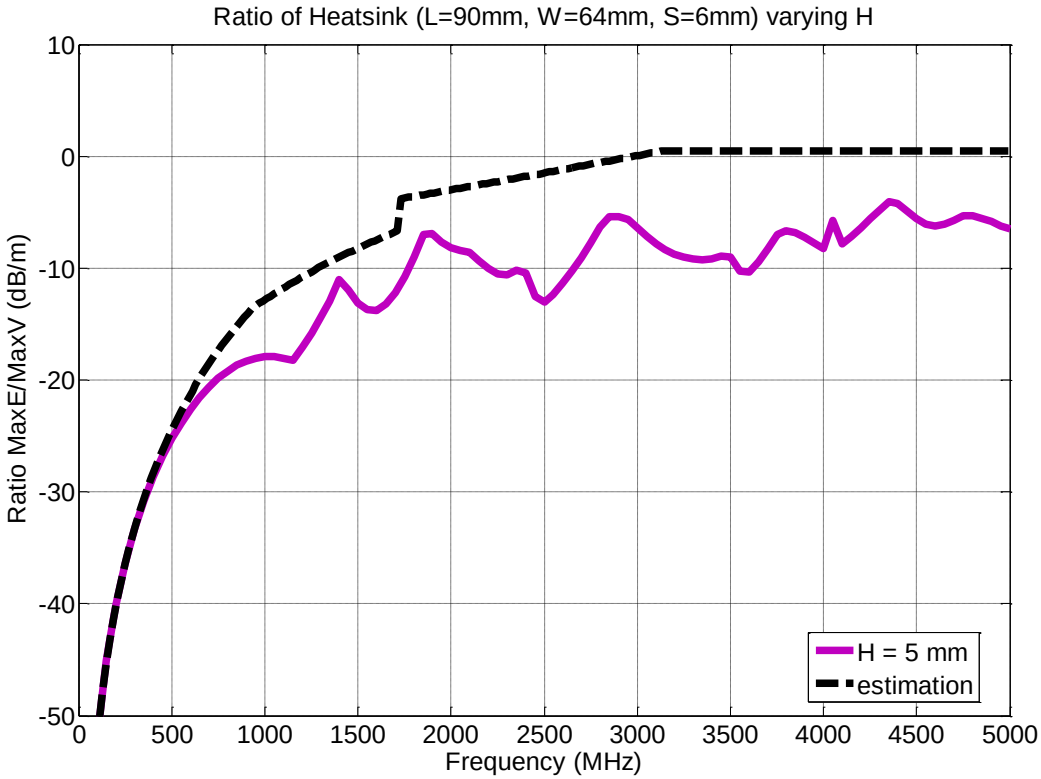

Fig. 14. Emissions from heatsink with dimensions: L=90 mm, W=64 mm, S=6 mm and H=5 mm.

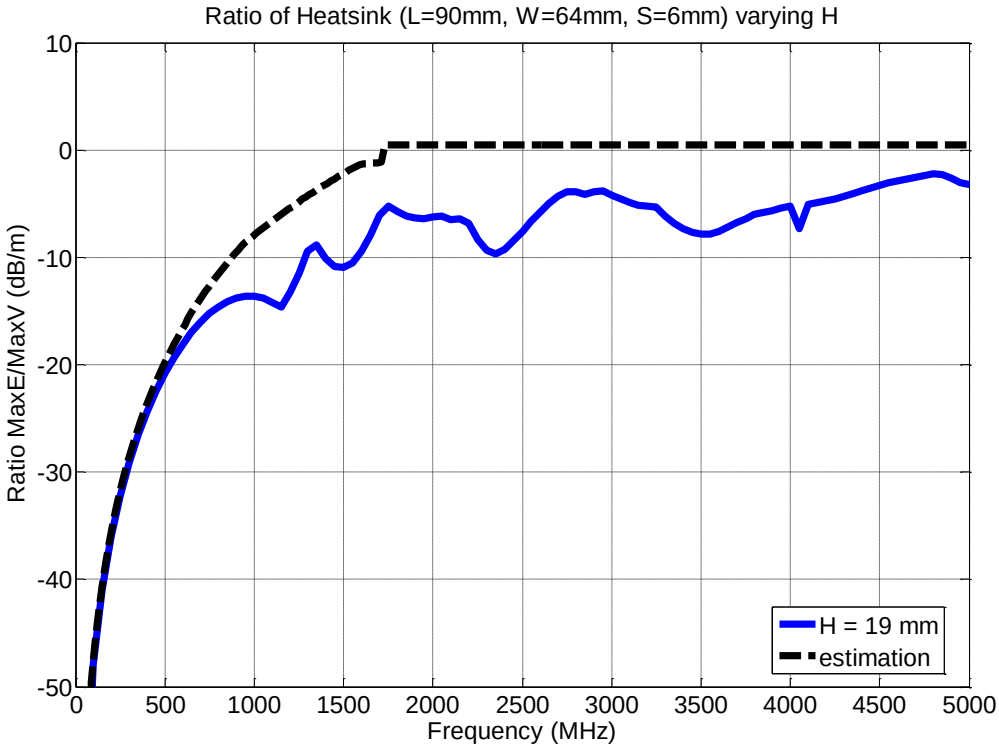

Fig. 15. Emissions from heatsink with dimensions: L=90 mm, W=64 mm, S=6 mm and H=19 mm.

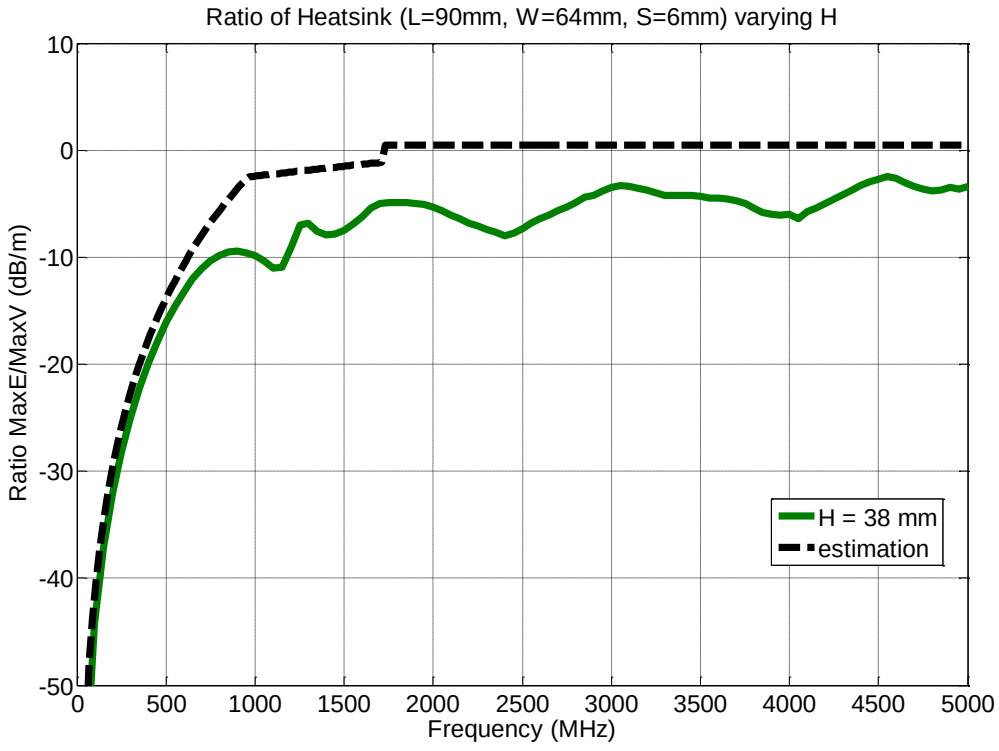

Fig. 16. Emissions from heatsink with dimensions: L=90 mm, W=64 mm, S=6 mm and H=38 mm.

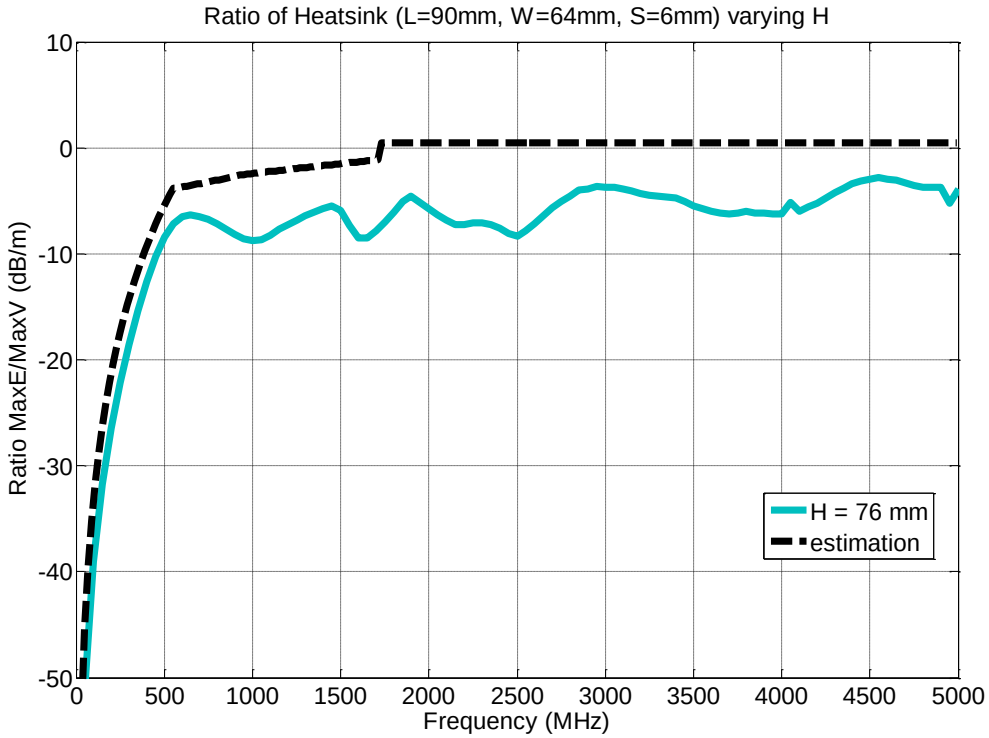

Fig. 17. Emissions from heatsink with dimensions: L=90 mm, W=64 mm, S=6 mm and H=76 mm.

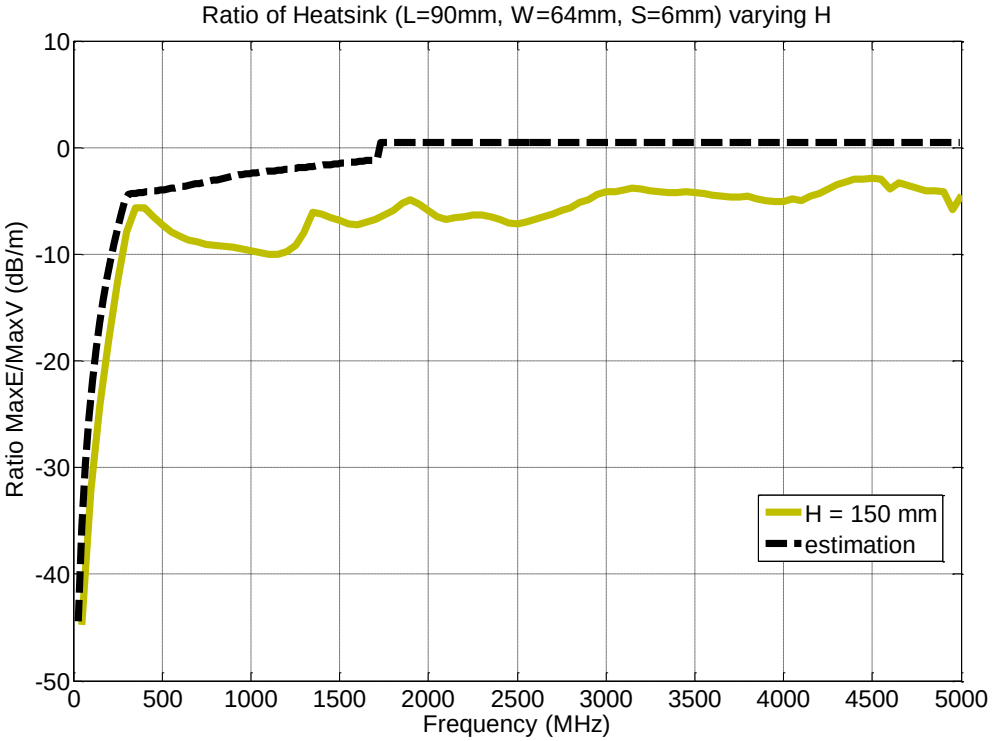

Fig. 18. Emissions from heatsink with dimensions: L=90 mm, W=64 mm, S=6 mm and H=150 mm.

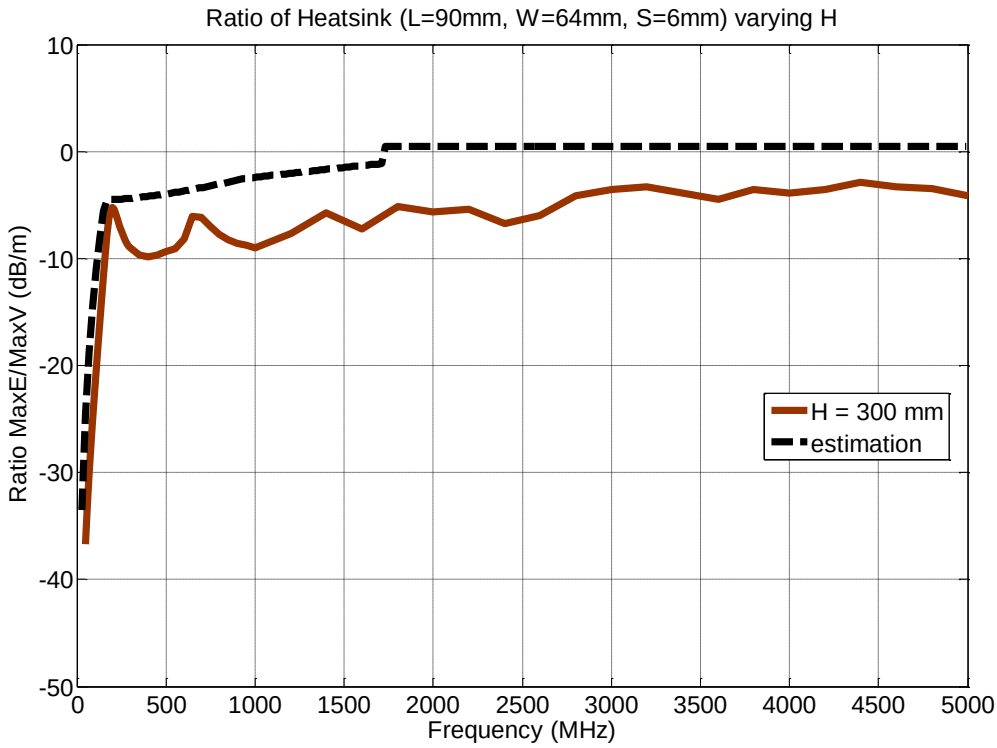

Fig. 19. Emissions from heatsink with dimensions: L=90 mm, W=64 mm, S=6 mm and H=300 mm.

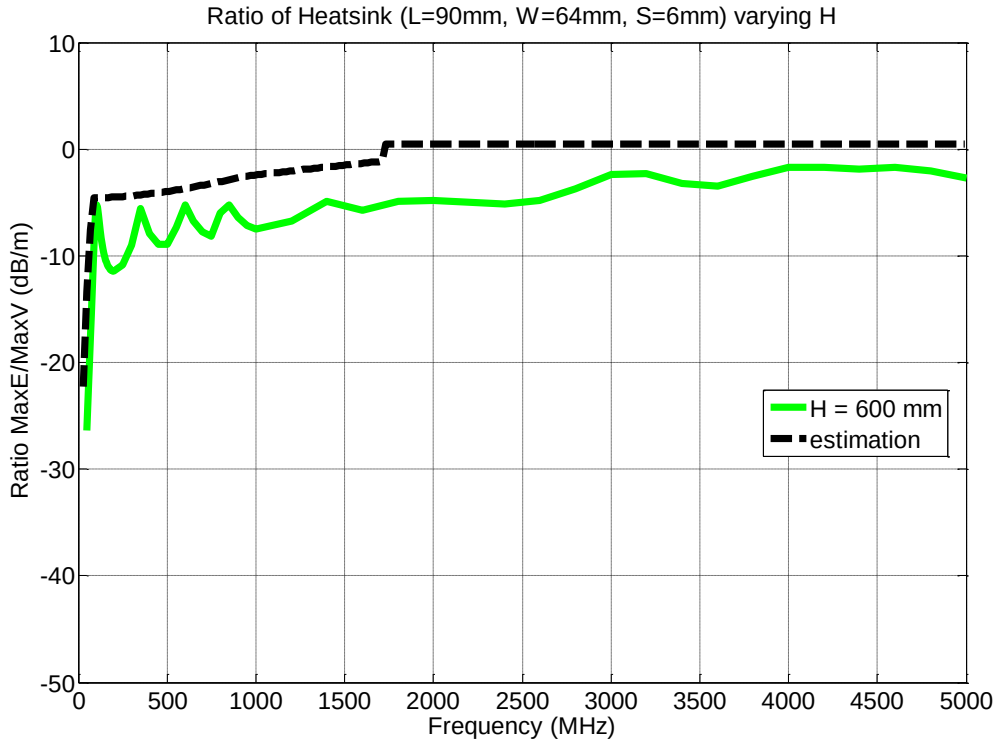

Fig. 20. Emissions from heatsink with dimensions: L=90 mm, W=64 mm, S=6 mm and H=600 mm.

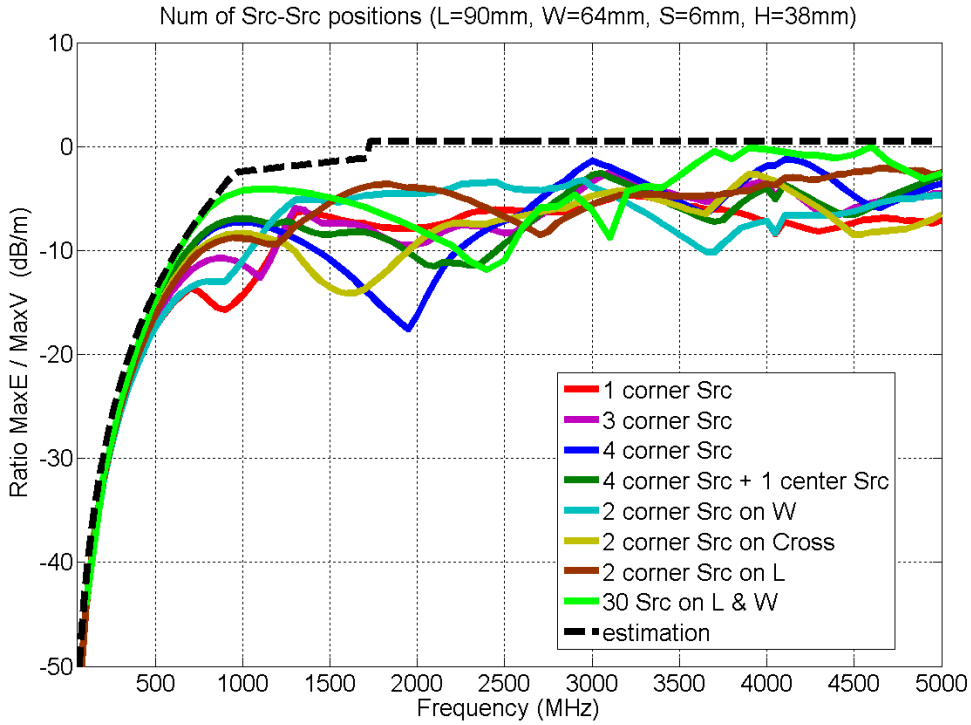

Fig. 21. Emissions from heatsink with dimensions: L=90 mm, W=64 mm, S=6 mm and H=38 mm.

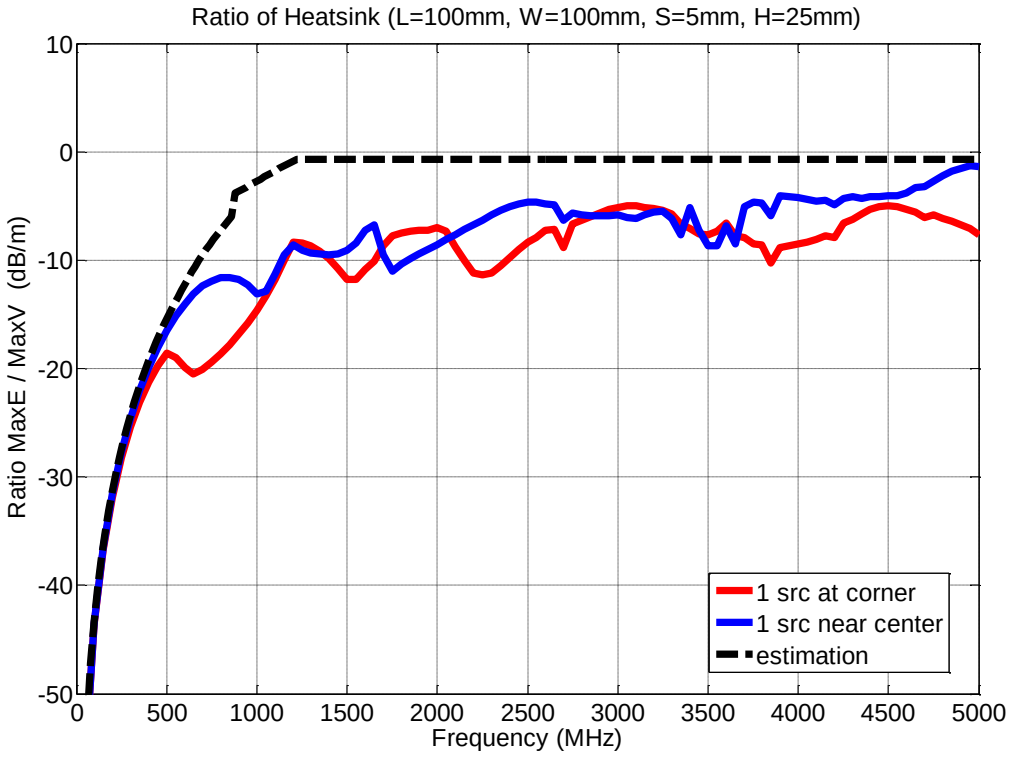

Fig. 22. Emissions from heatsink with dimensions: L=100 mm, W=100 mm, S=5 mm and H=25 mm.

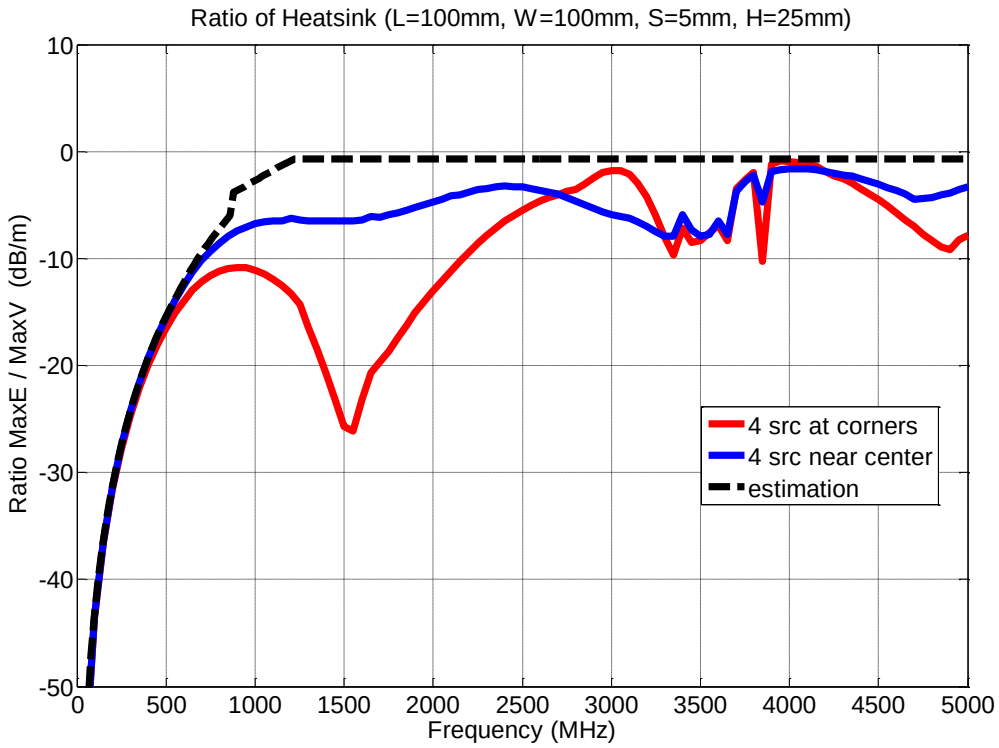

Fig. 23. Emissions from heatsink with dimensions: L=100 mm, W=100 mm, S=5 mm and H=25 mm.

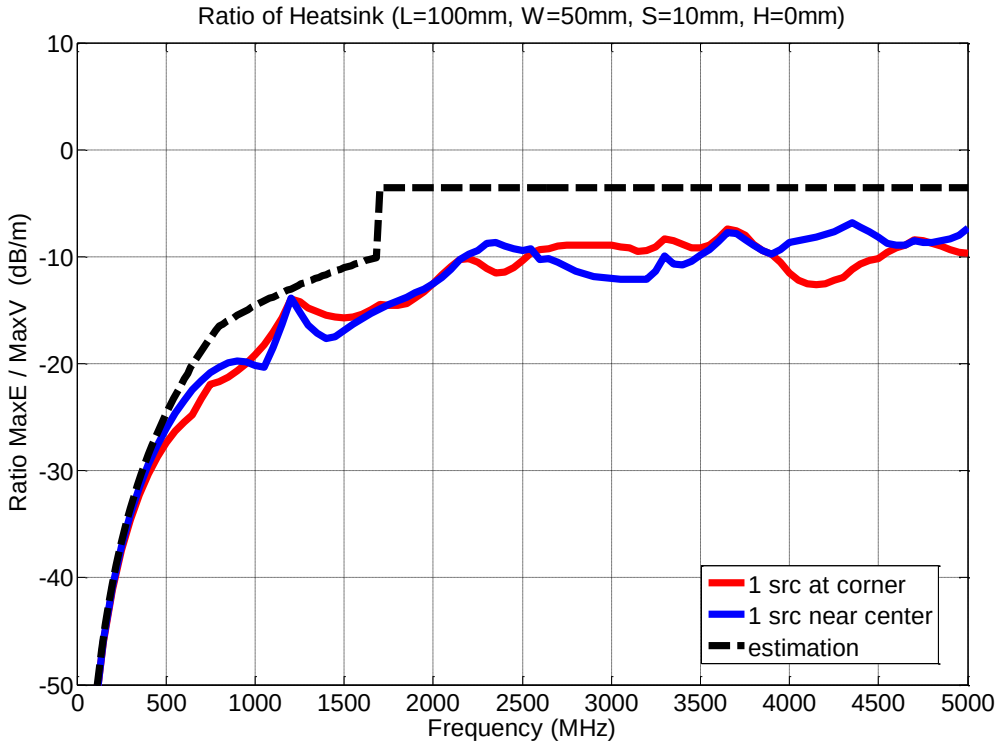

Fig. 24. Emissions from heatsink with dimensions: L=100 mm, W=50 mm, S=10 mm and H=0 mm.

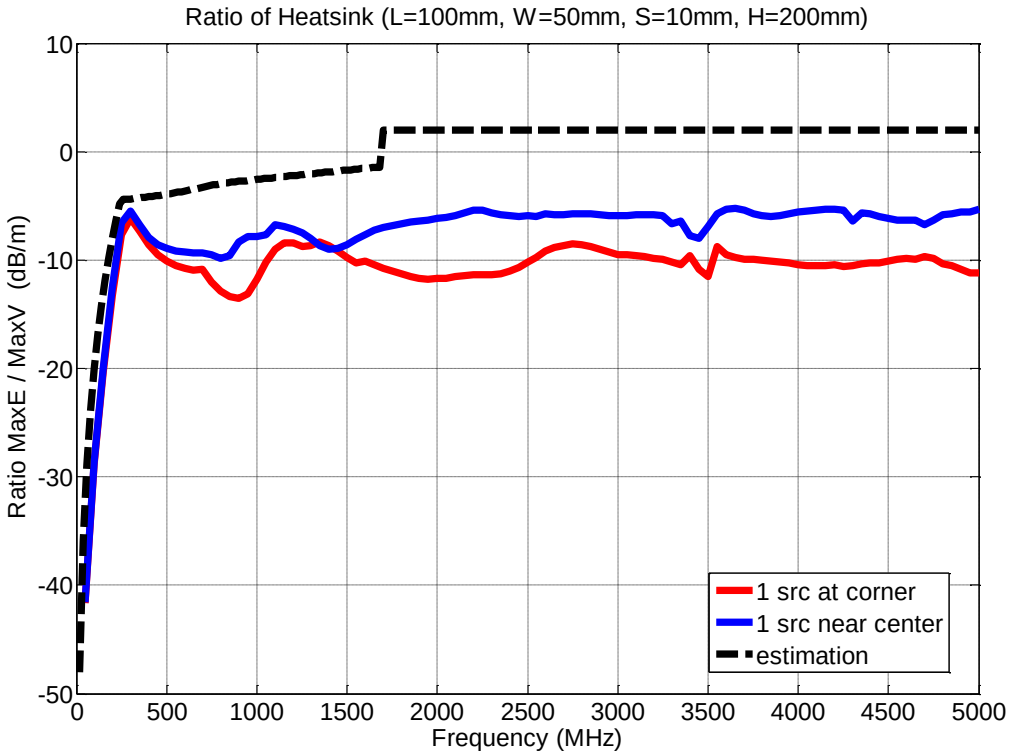

Fig. 25. Emissions from heatsink with dimensions: L=100 mm, W=50 mm, S=10 mm and H=200 mm.

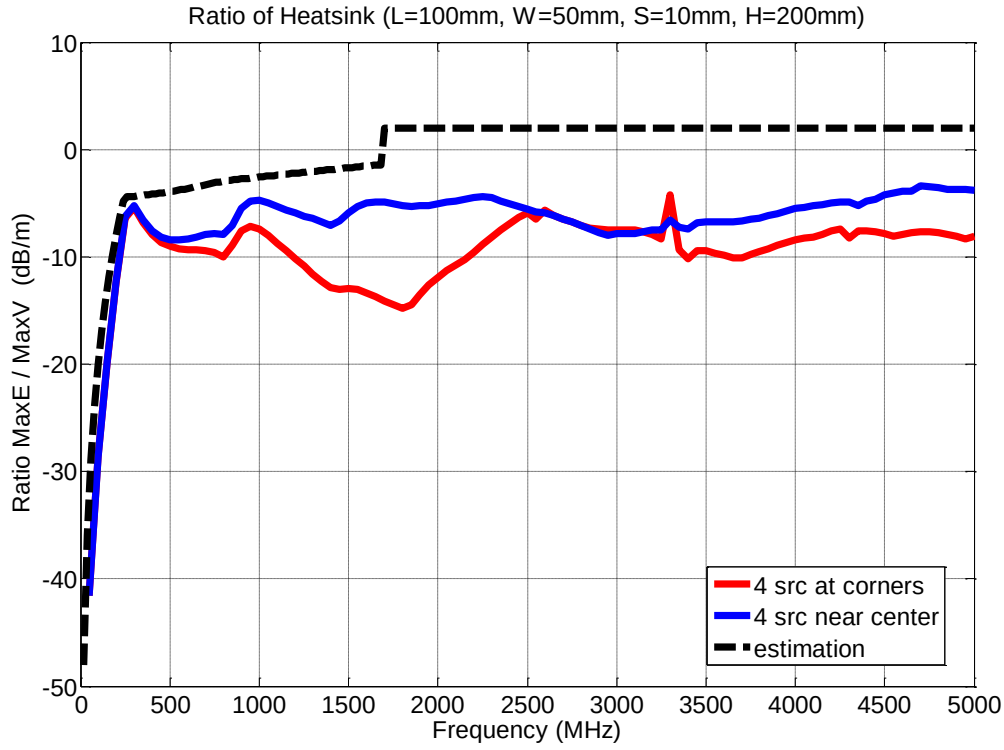

Fig. 26. Emissions from heatsink with dimensions: L=100 mm, W=50 mm, S=10 mm and H=200 mm.

5. Estimation of Heatsink Resonance Frequency

To estimate the first resonance frequency of a heatsink, the influence of the heatsink length and width should be considered. The heatsink resonance happens at a frequency lower than the frequency where the heatsink height is a quarter wavelength. If we view the heatsink's cross-section as extending the distance that current has to flow to reach the top center of the heatsink, we can postulate a new effective length for the heatsink. A formula for estimating the first resonance of a heatsink is proposed as,

$$f_{1st} = \frac{c_o}{4\left(H + S + \sqrt{L_{eff}^2 + W_{eff}^2}/2\right)}. \quad (3)$$

Where c_o is the free space light speed, H is the height of the heatsink, S is the cavity height, and L_{eff} and W_{eff} are the effective length and width of the cavity, respectively, when considering the edge effects of the cavity.

Table II. Tall heatsink 1st resonance frequency using two methods

Case #	Heatsink dimensions				Full-wave f_{1st} MHz	Formula (3) f_{1st} MHz
	Length mm	Width mm	Height mm	Spacing mm		
1	90	64	38	6	850	697
2	90	64	76	6	600	515
3	90	64	150	6	350	342
4	90	64	300	6	205	203
5	90	64	600	6	108	112
6	100	50	200	10	275	268

It is seen that this formula is very accurate when the heatsink height is relatively large compared to its length and width. It is not accurate when the heatsink is short. As can be observed from the simulation results, the cavity radiation dominates when the heatsink is relatively short. The radiation from the heatsink body is negligible, so the poor accuracy of (3) for a short heatsink does not affect the overall accuracy of the estimation equations (2a – 2c).

References

[1] C. F. Lee, K. Li, S. Y. Poh, R. T. Shin, and J. A. Kong, "Electromagnetic radiation from a VLSI package and heatsink configuration," *Proc. IEEE Int. Symp. Electromagn. Compat.*, pp. 393–398, Aug. 1991.

[2] K. Li, C. F. Lee, S. Y. Poh, R. T. Shin, J. A. Kong, "Application of FDTD method to analysis of electromagnetic radiation from VLSI heatsink configurations," *IEEE Trans. Electromagn. Compat.*, vol. 35, no. 2, pp. 204–214, 1993.

[3] Bruce Archambeault, Juan Chen, Satich Pratepeni, Lauren Zhang, David Wittwer, "Comparison of Various Numerical Modeling Tools Against a Standard Problem Concerning Heat Sink Emissions - Standard Modeling Paper 3," http://www.ewh.ieee.org/cmte/tc9/

[4] Y. Ji and T. Hubing, "EMAP5: A 3D Hybrid FEM/MOM Code," *Journal of the Applied Computational Electromagnetics Society*, vol. 15, no. 1, March 2000, pp.1-12.

[5] C. A. Balanis, *Antenna Theory: Analysis and Design, 3rd Edition*, Wiley-Interscience, Apr. 2005.

[6] X. He and T. Hubing, “A Closed-form Expression for Estimating the Maximum Radiated Emissions from a Heatsink on a Printed Circuit Board,” *Clemson Vehicular Electronics Laboratory Technical Report, CVEL-11-025*, April 9, 2011.